

**Oceanic dispersion
of radionuclides
along the coast of
Fukushima**

Y. Choi et al.

The impact of oceanic circulation and phase transfer on the dispersion of radionuclides released from the Fukushima Dai-ichi Nuclear Power Plant

Y. Choi, S. Kida, and K. Takahasi

Earth Simulator Center, Japan Agency for Marine-Earth Science and Technology, 3173-25 Showa-machi, Kanazawa-ku, Yokohama Kanagawa 236-0001, Japan

Received: 30 December 2012 – Accepted: 14 February 2013 – Published: 27 February 2013

Correspondence to: S. Kida (kidas@jamstec.go.jp)

Published by Copernicus Publications on behalf of the European Geosciences Union.

Title Page

Abstract

Introduction

Conclusions

References

Tables

Figures



Back

Close

Full Screen / Esc

Printer-friendly Version

Interactive Discussion

Abstract

The mechanism behind the dispersion of radionuclides released from the Fukushima Dai-ichi Nuclear Power Plant on March 2011 is investigated using a numerical model. This model is a Lagrangian particle tracking – ocean circulation coupled model that has the capability of solving the concentration of radionuclides for those dissolved in seawater and those adsorbed in particulates and bottom sediments. Model results show the radionuclides dispersing rapidly to the interior of the North Pacific along the Kuroshio Extension once they enter a meso-scale eddy. However, radionuclides are also found to remain near the coast with their spatial pattern depending strongly on the oceanic circulation during the first month of the release. This is when most of the adsorption to bottom sediments occurs. If the offshore advection were weak during this period, many radionuclides will be adsorbed to bottom sediments and remain on the coast for some time. If vertical mixing is weak, less radionuclide reach the sea floor and get adsorbed to bottom sediments. More radionuclides will then disperse to the open ocean.

1 The release of radionuclides from the coast of Fukushima

On March 2011, a significant amount of radionuclides were released to the ocean from the Fukushima Daiichi Nuclear Power Plant (hereafter FNPP) (Fig. 1). The amount of ^{137}Cs released is estimated to be about 3–27 PBq based on numerical models and observations (Kawamura et al., 2011; Bailly du Bois et al., 2011; Tsumune et al., 2012; Masumoto et al., 2012; Miyazawa et al., 2012a; Estournel et al., 2012), which is comparable to the amount that was released to the atmosphere (about 15 PBq, NERH, 2011). Recent studies, based on more rigorous calculation methods, tend to show an estimate around 5–6 PBq. Fukushima-origin radionuclides were also observed in the Kuroshio Extension region of the North Pacific in June 2011 (Buesseler et al., 2012). These observations suggest that some of the radionuclides have quickly dispersed to the open ocean within few months of its release from the coast. Observations show,

BGD

10, 3677–3705, 2013

Oceanic dispersion of radionuclides along the coast of Fukushima

Y. Choi et al.

Title Page

Abstract

Introduction

Conclusions

References

Tables

Figures

⏪

⏩

◀

▶

Back

Close

Full Screen / Esc

Printer-friendly Version

Interactive Discussion

however, high levels of radionuclides in seawater and sediments also near the coast (MEXT, 2011) and indicate that some of the radionuclides have not dispersed to the open ocean but remained there (Fig. 2).

What are the processes that control the dispersion of radionuclides near the Fukushima coast? Numerical models have been used to understand how the dispersion of radionuclides occurred in more detail, from local to the basin scale. Tsumune et al. (2011) used a coastal model and an Eulerian passive tracer model and showed that the radionuclides likely dispersed to the Sendai Bay to the coast of Ibaraki and the open ocean as east as 100 km from the FNPP (Fig. 1). Miyazawa et al. (2012b) used a nested high-resolution regional ocean model and an Eulerian passive tracer model to examine the impact of the wind, river outflow, and tides on the dispersion. They showed the radionuclides dispersing to the open ocean by April and suggested that oceanic circulation plays the dominant role. The wind is found to have a strong influence on the dispersion near the coast. Honda et al. (2012) used a Lagrangian particle tracking model based on oceanic surface currents and showed that radionuclides are capable of travelling as east as 155° E in a month or so.

While several studies have investigated the mechanism behind the dispersion of radionuclides near the Fukushima coast, modeling studies on the migration of radionuclides between seawater, particulate matter, and bottom sediments has been limited. Perianez et al. (2012) recently showed significant adsorption to bottom sediments near the FNPP but the spatial resolution and the coupling time scale with the oceanic model was moderate and thus the role of detailed flow field remains an open question. If the radionuclides are adsorbed to bottom sediments, they will likely remain on the sea floor near the coast for some time whereas if the radionuclides are dissolved in seawater or adsorbed in particulate matter, they will likely disperse to the open ocean with the seawater. Migration of radionuclides into different phases is therefore a major process that could decide whether the radionuclides will remain trapped near the coast or not. Since many biological activities take place along the coast, understanding the distribution of radionuclides there is important and observations do show higher level of radionuclides

BGD

10, 3677–3705, 2013

Oceanic dispersion of radionuclides along the coast of Fukushima

Y. Choi et al.

[Title Page](#)

[Abstract](#)

[Introduction](#)

[Conclusions](#)

[References](#)

[Tables](#)

[Figures](#)

[⏪](#)

[⏩](#)

[◀](#)

[▶](#)

[Back](#)

[Close](#)

[Full Screen / Esc](#)

[Printer-friendly Version](#)

[Interactive Discussion](#)



even after few months after its release (Fig. 2). This motivates us to examine how phase transfer of radionuclides may have played a role on the dispersion of radionuclides.

In this paper, we will investigate the process responsible for the dispersion of radionuclides near the Fukushima coast using a Lagrangian particle-tracking model, which is coupled to a high resolution ocean circulation model. The particle-tracking model is capable of solving the migration of radionuclides between three phases; dissolved phase, particulate phase, and bottom sediment phase, which is the main focus of this study. By coupling the particle-tracking model to a high-resolution ocean numerical model, we anticipate that the turbulent flow field of the region is realistically resolved as well. The details of the model setup will be described next in Sect. 2. The simulation results are then presented and compared with observations in Sect. 3. The sensitivity of the dispersion to the magnitude of vertical mixing is examined in Sect. 4. Summary and discussion are presented in Sect. 5.

2 Description of the ocean – particle tracking coupled model

A regional numerical ocean circulation model is used to simulate the flow field near the coast of Fukushima and a Lagrangian particle-tracking model uses this flow field to solve the movement and migration of radionuclides into different phases. The coupling between the two models occurs every 30 min and the model is integrated from 1 December 2010 to 30 June 2011.

2.1 Ocean circulation model

The oceanic component of the Multi-Scale Simulator for the Geo-environment (MSSG) is used for the ocean circulation model (Kida, 2011). This numerical ocean model is a z-coordinate model with a non-hydrostatic capability but we will use the hydrostatic option here. The model domain covers 140.2° E to 143.2° E and 34.85° N to 39.14° N with a horizontal grid spacing of about 2 km (Fig. 3). High spatial resolution is used in

BGD

10, 3677–3705, 2013

Oceanic dispersion of radionuclides along the coast of Fukushima

Y. Choi et al.

Title Page

Abstract

Introduction

Conclusions

References

Tables

Figures

⏪

⏩

◀

▶

Back

Close

Full Screen / Esc

Printer-friendly Version

Interactive Discussion

Oceanic dispersion of radionuclides along the coast of Fukushima

Y. Choi et al.

[Title Page](#)

[Abstract](#)

[Introduction](#)

[Conclusions](#)

[References](#)

[Tables](#)

[Figures](#)

[⏪](#)

[⏩](#)

[◀](#)

[▶](#)

[Back](#)

[Close](#)

[Full Screen / Esc](#)

[Printer-friendly Version](#)

[Interactive Discussion](#)

order to resolve the eddy-rich flow field because such feature is an essential part of the dynamics in the region. The coast of Fukushima is located in the Kuroshio-Oyashio Interfrontal Zone (Yasuda, 2003) where two western boundary currents collide and intense meso-scale eddies are generated. Bottom depths (D) are a spatial average of ETOPO1 (Amante and Eakins, 2009) with 73 levels in the vertical with 3 m resolution near the surface to 250 m near the bottom.

The lateral boundaries of the flow field, temperature and salinity are set to the daily outputs of the Japan Coastal Ocean Predictability Experiment (JCOPE)-2, a data assimilated product of the region with a resolution of $1/12^\circ$ (Miyazawa et al., 2009). JCOPE2 is known to assimilate the pathway of the Kuroshio well and we thus believe that its outputs are reasonably close to reality. There is a sponge layer of about 40 km around the lateral boundaries to adjust the simulated flow field smoothly to that of JCOPE2 output.

Surface temperature and salinity are restored to that of JCOPE2 outputs with a restoring time scale of 1 day. While we understand that this is rather strong restoring time scale, we chose to match it with that of the JCOPE2 output frequency. Surface wind stress is estimated using Large and Pond (1981) from 10 m wind of the Grid Point Value of Meso-Scale Model (GPV/MSM) that is provided by the Japan Meteorological Agency every 6 h and has a high horizontal resolution of about 0.05 degrees. For the subgrid scale parameterization, Smagorinsky-type Laplacian viscosity and diffusion is used with a coefficient of 0.4 in the lateral direction. Noh-Kim vertical mixing scheme is used for vertical viscosity and diffusion (Noh and Kim, 1999).

2.2 Lagrangian particle-tracking model

A Lagrangian model is used to solve the concentration of radionuclides since such coordinate system is natural to the movement of particles in the ocean. The model is originally used for oil-spilling accidents (Choi et al., 2011, 2013) but we have modified the equations so that they are better suited for radionuclides. The dispersion of

radionuclides is solved three-dimensionally based on the following equations:

$$\frac{dC_{\text{diss}}}{dt} = Q - k_1 C_{\text{diss}} + k_2 C_{\text{LPM}} - k_3 C_{\text{diss}} + \phi k_2 C_{\text{sed}} \quad (1)$$

$$\frac{dC_{\text{LPM}}}{dt} = +k_1 C_{\text{diss}} - k_2 C_{\text{LPM}} - \text{Set} + \text{Ero}, \quad \text{and} \quad (2)$$

$$\frac{dC_{\text{sed}}}{dt} = +k_3 C_{\text{diss}} - \phi k_2 C_{\text{sed}} + \text{Set} - \text{Ero} \quad (3)$$

C_{diss} , C_{LPM} , and C_{sed} are the concentration of radionuclides that are dissolved in sea-water, adsorbed in large particulate matter (LPM) (particulates with a diameter between 0.5–62.5 μm), and adsorbed in bottom sediments, respectively. We will refer to these three phases as radionuclides in dissolved phase, LPM phase, and bottom sediment phase, hereafter. d/dt is the time derivative following the particle. Q is the source term. Terms with k_n are the phase transition terms. Set is the settling from LPM phase to bottom sediment phase occurring at the sea floor and Ero is the erosion from bottom sediment phase to LPM phase. Equations (1)–(3) are roughly equivalent to that used in Periàñez (2000) and the schematic of the processes involved are shown in Fig. 3a. Note that we have neglected the decaying process because the half-life of 30 yr for ^{137}Cs is significantly longer than the model integration time pursued in this study.

We have assumed that the radionuclides in dissolved phase does not sink vertically and that those in LPM phase sink with a settling velocity of w_s ($= -2 \times 10^{-4} \text{ms}^{-1}$). The radius of LPM is assumed to be about 15 μm . The radionuclides in bottom sediment phase will sit on the seabed and not get advected. Settling and erosion occur only at the bottom. The radionuclides in dissolved phase follow the movement of seawater so the oceanic flow field (u_o) is used for its pathway, $u = (u_o, v_o, w_o)$. On the other hand, the radionuclides in LPM phase follow the movement of seawater as it sink with the settling velocity so its pathway is $u = (u_o, v_o, w_o + w_s)$. While the settling velocity of suspended particles is often expressed by a function of suspended matter concentration or diameter of particles (e.g. Mehta, 1989; Nicholson and O'Connor, 1986; Sternberg et al., 1999), we have chosen to use a single value following Kobayashi et al. (2007).

**Oceanic dispersion
of radionuclides
along the coast of
Fukushima**

Y. Choi et al.

Title Page

Abstract

Introduction

Conclusions

References

Tables

Figures

⏪

⏩

◀

▶

Back

Close

Full Screen / Esc

Printer-friendly Version

Interactive Discussion



The oceanic flow field will be represented by $u_o = u_m + u'$, where u_m is the simulated flow field in the ocean model and u' is the turbulent flow field in the subgrid scale. u' is added because the ocean model does not explicitly solve the subgrid scale motion and uses eddy diffusivity. Here, u' will be represented in the form of a random walk following Periañez (2000):

$$u' = R \cos \vartheta \cdot \sqrt{\frac{12A_H}{\Delta t}}, \quad (4)$$

$$v' = R \cos \vartheta \cdot \sqrt{\frac{12A_H}{\Delta t}}, \quad \text{and} \quad (5)$$

$$w' = R \sqrt{\frac{2A_V}{\Delta t}}. \quad (6)$$

R is a random number between -1 and 1 . ϑ is a random angle between 0 to π . The horizontal diffusivity coefficient A_H , and vertical diffusivity coefficient A_V , are those that are calculated in the ocean model.

Q is prescribed based on the idealized discharge time series presented in Tsumune (2012) (Fig. 3b). Total input is adjusted to 5.5 PBq so that it is within the range estimated in recent studies (e.g. Masumoto et al., 2012). This idealized source term has at a constant rate of 3.3 TBq day^{-1} from 26 March to 6 April but decreases exponentially to $0.033 \text{ TBq day}^{-1}$ after 6 April and then remains constant up to 31 May. Source term is zero beyond 31 May. Radionuclides are added to a 1.0 km (meridional) \times 500 m (zonal) \times 5 m (from the surface) boxed region next to the FNPP with each particles representing 10^{10} Bq of radionuclides.

The values and expressions for the phase transfer, settling, and erosion described above are based on those used by past studies (Periañez, 2000; Periañez and Elliott, 2002; Kobayashi et al., 2007) unless noted. The phase transition terms are calculated based on a stochastic method: radionuclides are transferred from one phase to another

BGD

10, 3677–3705, 2013

Oceanic dispersion of radionuclides along the coast of Fukushima

Y. Choi et al.

Title Page

Abstract

Introduction

Conclusions

References

Tables

Figures



Back

Close

Full Screen / Esc

Printer-friendly Version

Interactive Discussion



Oceanic dispersion of radionuclides along the coast of Fukushima

Y. Choi et al.

[Title Page](#)

[Abstract](#)

[Introduction](#)

[Conclusions](#)

[References](#)

[Tables](#)

[Figures](#)

[⏪](#)

[⏩](#)

[◀](#)

[▶](#)

[Back](#)

[Close](#)

[Full Screen / Esc](#)

[Printer-friendly Version](#)

[Interactive Discussion](#)

with a probability of $1 - \exp^{-k_n \Delta t}$. Terms with k_1 , k_2 , k_3 and φk_2 represent the adsorption from dissolved to LPM phase, desorption from LPM to dissolved phase, adsorption from dissolved to bottom sediment phase, and desorption from bottom sediments to dissolved phase, respectively. k_1 is set to $(200 \text{ day})^{-1}$ and is estimated assuming that the LPM concentration is about 0.1 mg L^{-1} . Because such concentration values is unclear for the coast of Fukushima, a value based on observations near the coast in the North Sea (van Raaphorst et al., 1998) is used, where it is shallow, have similar magnitude of tidal currents, and is an opened sea like the coast of Fukushima. k_2 is set to $(1.0 \text{ day})^{-1}$ and φ is set to 0.1. Adsorption from dissolved to sediment phase occur only when the particulate reach the bottom and k_3 is expressed as an inverse function of depth $(= 4.2 \times 10^{-5} / D [\text{s}])$. Its magnitude would be about $(5 \text{ days})^{-1}$ where 20 m deep but more than $(30 \text{ days})^{-1}$ where deeper than 100 m. Settling occurs once the radionuclides land on the sea floor. Erosion is a function of bottom flow speed $(= 2.4 \times 10^{-4} |u|^{3.4})$ and increases with the bottom current. While these modeling parameters are based on past studies, there are likely to be differences for each sea as well as spatial variability within the sea. However, the specific values appropriate for the coast of Fukushima are unknown. We therefore use these values based on past modeling studies and observations and aim to capture and understand the processes involved in the dispersion or radionuclides to its first order.

The numerical experiments based on the setup as described above will be referred to as CTRL hereafter. To test the sensitivity of the dispersion to the magnitude of vertical mixing, we have also pursued an experiment where the vertical mixing coefficient in the particle-tracking model is set an order smaller than the values simulated in CTRL. This experiment will be referred to as SMIX hereafter. The magnitude of the vertical mixing coefficient can vary significantly due to the actual weather, seasons, and biological conditions and so we will examine how much these factors may affect the simulation results. As we will show later on, the magnitude of the vertical mixing has a strong impact on the adsorption to bottom sediments and affects the dispersion of radionuclides to the open ocean.

2.3 Observational products

Model simulations are compared with the monthly averages of in-situ observations for radionuclide in seawater and bottom sediments near the Fukushima coast. These observation data are provided by TEPCO, Ministry of Education, Culture, Sports, Science and Technology (MEXT), Ministry of the Environment (ME), and Fukushima Prefecture (FP) through the MEXT website (<http://radioactivity.mext.go.jp>) (MEXT, 2011). Observations of radionuclides in bottom sediments shown in Fig. 2 are drawn from this data set and most of the observations are near the coast of the FNPP. Observations by TEPCO are measured by [Bqkg⁻¹ wet] while others are [Bqkg⁻¹ dry]. Data provided by TEPCO are therefore shown in triangles to clarify this difference. The values are also converted to [Bqkg⁻¹ dry] by multiplying 0.75, which is the average dry/wet ratio observed near the coast of Fukushima (MEXT, 2011). Such ratio obviously differs for each location but our aim is to get the first order picture on the magnitude and the spatial variability of radionuclides adsorbed to bottom sediments. Satellite imageries of surface temperature by the Moderate-Resolution Imaging Spectroradiometer (MODIS) are also used for evaluating the spatial structure of the flow field in the region. This product has a spatial resolution of 4 km and has better spatial resolution than the sea surface height from AVISO. Although MODIS data is sometimes contaminated by the clouds, it shows good spatial coverage roughly every week.

3 The simulated oceanic flow field and the dispersion of radionuclides

We will first describe the surface flow field simulated in CTRL. The radionuclides that are simulated using this oceanic flow will then be described. What we find is that in the presence of migration from dissolved phase to LPM phase and to bottom sediment phase, a significant amount of the radionuclides remain close to the coast even after few months from its release.

BGD

10, 3677–3705, 2013

Oceanic dispersion of radionuclides along the coast of Fukushima

Y. Choi et al.

Title Page

Abstract

Introduction

Conclusions

References

Tables

Figures

⏪

⏩

◀

▶

Back

Close

Full Screen / Esc

Printer-friendly Version

Interactive Discussion

3.1 The oceanic flow field

The flow field near the Fukushima coast shows a weak northeastward flow from March to April that flows along the 100 m bathymetric contour line (Fig. 4a–c). This northward flow appears to strengthen gradually in April, bring warm SST water, and create a SST front west and east side of this flow. Such SST fronts are found in observations as well (Fig. 5a–c). While the weekly averaged flow shows a general northeastward flow, the flow field has significant variability and a southward flow is occasionally found along the coast of FNPP in late March (Fig. 4a). This southward flow advects the cold SST water from the northern Sendai Bay and is likely to be partly responsible for creating the SST front near the coast. The flow field much off-shore of Fukushima shows a south-eastward flow from March to April. However, the flow field of this region is also highly variable and is associated with many meso-scale eddies.

The flow field near Ibaraki shows the presence of an anti-cyclonic eddy from March to April (Fig. 4a–c). The center of this eddy is located around 36.2° N and 141.4° E with a size of about 100 km. The presence of an eddy of such size with a warmer SST than that near the coast is indeed observed although the signal is slightly weaker in the observations (Fig. 5a–c). The anti-cyclonic eddy in the model begins to merge with the Kuroshio Extension in late April (Fig. 4c) and then completely merge by mid-May (Fig. 4d). However, the eddy appears to reestablish itself in late May when the Kuroshio Extension shifts south. The center of the anti-cyclonic eddy found in June is now located around 36.6° N and 141.7° E, which is slightly northward and eastward than that found in April.

For a few days at the end of May, the flow along the coast of Fukushima and Ibaraki abruptly becomes a strong southward flow (Fig. 4e) This is when an extra-tropical cyclone passes over the region. The strong easterly wind forces an accumulation of water near the coast and induces the southward flow that is as fast as 1.8 ms⁻¹. The SST also cools along the coast, and such narrow signal can be recognized in observations as well (Fig. 5e). The advection of cold SST water from the north is also likely important

BGD

10, 3677–3705, 2013

Oceanic dispersion of radionuclides along the coast of Fukushima

Y. Choi et al.

Title Page

Abstract

Introduction

Conclusions

References

Tables

Figures

⏪

⏩

◀

▶

Back

Close

Full Screen / Esc

Printer-friendly Version

Interactive Discussion

for creating the cold SST field along the coast. The use of SST nudging, however, may have weakened the narrow and cold structure along the coast compared to observations since JCOPE2 has lower spatial resolution than our model. The region warms up by late June and the SST front near the coast is weakened (Figs. 4f and 5f).

5 3.2 The dispersion of radionuclides

Radionuclides in dissolved phase and LPM phase move roughly along with seawater so their spatial distribution will be described together. The behavior of the radionuclides in these two phases is the one that can be compared with past studies where radionuclides are treated as a passive tracer and phase transfers do not occur.

10 3.2.1 Radionuclides in seawater

Soon after the major release of radionuclides, radionuclides in seawater (dissolved phase and LPM phase) move south for a few days because a southward flow is simulated along the coast at that time. However, the radionuclides eventually move north, following the average northward flow field from March to April (Fig. 6a, b). A significant north–south asymmetry thus establishes. Many of the radionuclides also spread inside the Sendai Bay (Fig. 6c), where the topography is shallow, and the northerly wind from March to early April is likely behind such dispersion because northerly wind forces a westward surface Ekman transport. The northerly wind weakens by late-April and the radionuclides appear to spread following the northward oceanic flow that exists along the bathymetric lines of about 100 ~ 200 m. By the end of April, the wind turns south and the surface Ekman transport reverses towards the east. The radionuclides then begin to spread to the open ocean in May as they move anticyclonically following the oceanic flow field (Fig. 6d).

25 The meridional asymmetry weakens abruptly at the end of May when an extra-tropical cyclone crosses over Japan and induces a strong southward flow along the coast of Ibaraki (Fig. 6e). This strong southward flow brings a significant amount of

BGD

10, 3677–3705, 2013

Oceanic dispersion of radionuclides along the coast of Fukushima

Y. Choi et al.

Title Page

Abstract

Introduction

Conclusions

References

Tables

Figures

⏪

⏩

◀

▶

Back

Close

Full Screen / Esc

Printer-friendly Version

Interactive Discussion

radionuclides towards the south of the FNPP and weakens the meridional asymmetry for a few days. However, the radionuclides that are advected along the coast of Ibaraki do not reach the southern tip of Ibaraki where the Kuroshio Extension exists so the radionuclides are unlikely to disperse directly to the open ocean there. The majority of the radionuclides are dispersing to the interior of the North Pacific east of the FNPP where an anti-cyclonic eddy advects the radionuclides towards the Kuroshio Extension (Fig. 6d–f).

3.2.2 Radionuclides in bottom sediment phase

We find the majority of the radionuclides adsorbed in bottom sediments where it is shallow (< 100 m) (Fig. 7a–f). While the transfer rate from dissolved to LPM phase is small, the magnitude of the source is large and will create decent amount of radionuclides in LPM phase. When these radionuclides are near the bottom, they will settle on the sea floor and transfer to bottom sediment phase. Note that in order to make the comparison between the model results and observations easier, model results are converted from $[\text{Bq m}^{-2}]$ to $[\text{Bq kg}^{-1} \text{ dry}]$ in the figures. We have assumed that the bulk density of bottom sediments is 900 kg m^{-3} and that the radionuclides are trapped within the top 10 cm from the sea floor, thus $[\text{Bq kg}^{-1} \text{ dry}] = 1/(0.1 \cdot 900) [\text{Bq m}^{-2}]$. Phase transfer from dissolved or LPM to bottom sediment phase occur only at the bottom so the radionuclides that are released at the surface need some time to descend to the bottom. For a water column about 50 m deep and with a vertical mixing coefficient of about $1 \times 10^{-2} \text{ m}^2 \text{ s}^{-1}$, it only takes 2–3 days for the radionuclides to reach the bottom and adsorb to bottom sediments. For the radionuclides that are advected to where the topography is more than 200 m deep, however, it would take more than a month for them to adsorb to bottom sediments even if vertical mixing coefficient is as large as $1 \times 10^{-2} \text{ m}^2 \text{ s}^{-1}$ from the surface to the bottom. Since the surface mixed layer with a vertical mixing coefficient of the order $10^{-2} \text{ m}^2 \text{ s}^{-1}$ is limited to the top 100 m at the most we consider it reasonable that the model does not show much accumulation of radionuclides where the topography is more than 100 m deep. We find the changes in the magnitude of the

Oceanic dispersion of radionuclides along the coast of Fukushima

Y. Choi et al.

Title Page

Abstract

Introduction

Conclusions

References

Tables

Figures

⏪

⏩

◀

▶

Back

Close

Full Screen / Esc

Printer-friendly Version

Interactive Discussion



settling velocity to increase the amount of radionuclides in bottom sediment phase but not affect the spatial distribution simulated in the model qualitatively.

The spatial distribution of radionuclides in bottom sediment phase shows high values near the source but it also reflects the meridional asymmetry found in dissolved phase and LPM phase; more radionuclides are found in Sendai bay than along the coast of Ibaraki (Fig. 7a–d). Accumulation occurs along the coast of Ibaraki at the end of May, when the strong southward flow advects the radionuclides from the north (Fig. 7e). However, the duration of the southward flow is only for a few days and is short, so the accumulation there is small compared to the Sendai Bay (Fig. 7f).

Although the number of observation points is limited, the magnitude and the spatial distribution of radionuclides appears to agree reasonably well with that observed for those in seawater (Fig. 6g–i) and bottom sediments (Fig. 7g–i) The increase in the dispersion of the dissolved and LPM phases to the open ocean simulated for June in the model (Fig. 6c–f) matches with the general increase in the off-shore values in the observations (Fig. 6h, i). The concentration of radionuclides in seawater found in the Kuroshio Extension region is also similar magnitude as that observed (Buesseler et al., 2012). Higher concentration found to the north of the FNPP but with an increase in concentration to the south of FNPP from May to June is observed for both seawater and bottom sediments (Fig. 7h, i). This is in accordance with the advection of radionuclides that are simulated along the Ibaraki coast when a southward flow establishes at the end of May (Figs. 6e and 7e). High concentration values observed in seawater about 30 km offshore of the FNPP in April (Figs. 6g and 7g) is not simulated in our model but as past studies have shown (e.g. Tsumune et al., 2011), these high values are likely due to atmospheric deposits and not the oceanic flow.

3.2.3 Time dependence

The time series showing the number of radionuclides in each phase show gradual adsorption of radionuclides from dissolved phase to bottom sediment phase after the radionuclides are introduced on 26 March (Fig. 8a). This accumulation in bottom

BGD

10, 3677–3705, 2013

Oceanic dispersion of radionuclides along the coast of Fukushima

Y. Choi et al.

Title Page

Abstract

Introduction

Conclusions

References

Tables

Figures

⏪

⏩

◀

▶

Back

Close

Full Screen / Esc

Printer-friendly Version

Interactive Discussion



Oceanic dispersion of radionuclides along the coast of Fukushima

Y. Choi et al.

[Title Page](#)

[Abstract](#)

[Introduction](#)

[Conclusions](#)

[References](#)

[Tables](#)

[Figures](#)

[⏪](#)

[⏩](#)

[◀](#)

[▶](#)

[Back](#)

[Close](#)

[Full Screen / Esc](#)

[Printer-friendly Version](#)

[Interactive Discussion](#)

sediment phase begins after few days, which matches well with the time scale of radionuclides reaching the bottom from the surface through vertical mixing. As mentioned earlier, when mixing coefficient is on the order of $10^{-2} \text{ m}^2 \text{ s}^{-1}$, its time scale is only a few days for a 50 m deep ocean. While the transfer rate from dissolved to LPM is slow, significantly large initial concentration near the source as well as the strong vertical mixing near the surface enables these accumulation of radionuclides in bottom sediment phase. By late April, a month after the major release of the radionuclides, most of the adsorption has taken place and about 0.43 PBq are found to remain in bottom sediment phase near the coast. Gradual accumulation in bottom sediment phase is observed in the shallow regions ($< 50 \text{ m}$) in May but desorption from sediment to dissolved phase also begins to increase. A strong erosion event is simulated at the end of May, which will decrease the bottom sediment phase and increase the dissolved and the LPM phase. This occurs when the strong southward flow is induced by the extra-tropical cyclone. Dispersion towards the open ocean occurs gradually from May. By late June, about 1 PBq of radionuclides are found in the open ocean ($> 200 \text{ m}$). Those in the bottom sediment phase appear to decrease slightly compared to early June.

The majority of the adsorption of radionuclides to bottom sediments and its spatial variability appears to be decided during the first 30–40 days or so. This suggests that the oceanic flow field during this period has a profound impact on the spatial distribution of radionuclides for much longer time scale. For the radionuclides from the FNPP, the northward flow and the northerly wind during March to April are likely responsible for creating the meridional asymmetry in the distribution of radionuclides and prevent radionuclides from dispersing to the open ocean (Figs. 6 and 7). If the offshore motion is weak during the first month, more adsorptions of radionuclides to bottom sediments will occur because the radionuclides are in the shallow seas. Once the adsorption to bottom sediments occur, the radionuclides are likely to remain along the coast for some time. On the other hand, if the offshore advection were strong during the first month from the release, more radionuclides are likely to disperse to the open ocean where the adsorption to bottom sediments is much limited.

4 The impact of vertical mixing

CTRL showed a significant amount of radionuclides remaining in the bottom sediments along the coast of Fukushima even after few months after their release. We will next examine the sensitivity of the results to the vertical mixing coefficient by comparing CTRL with SMIX.

4.1 The spatial structure of the dispersion

We find the basic spatial variability of the dispersion similar to CTRL (Figs. 6a–f, 7a–f) for those in dissolved and LPM phases (Fig. 9a–c) and those in bottom sediment phase (Fig. 9d–f). Northward advection of radionuclides occurs in April and the off-shore dispersion strengthens in May and June. This is because the dispersion of radionuclides for dissolved and LPM phases are determined mostly by the oceanic flow and the wind, which is the same for CTRL and SMIX. The distribution of the radionuclides in bottom sediment phase follows those in dissolved and LPM phases in the shallow regions so SMIX also shows similar behavior. The differences are that the concentration of radionuclides in dissolved and LPM phases in the open ocean are much higher and more widely spread in SMIX than in CTRL (Figs. 6e and 9b). For those in bottom sediment phase, the concentrations are found to be generally close to CTRL and the differences are more complex. The values found near the FNPP show dramatic decrease from CTRL to SMIX while off-shore values show slightly larger values; concentrations found in Sendai Bay in May–June are somewhat higher in SMIX than in CTRL. Such differences likely arise because the radionuclides take longer time to reach the bottom in SMIX. Then the radionuclides are capable of being advected away from the source by the time they reach the bottom, making desorption limited near the source but enhanced further away.

BGD

10, 3677–3705, 2013

Oceanic dispersion of radionuclides along the coast of Fukushima

Y. Choi et al.

Title Page

Abstract

Introduction

Conclusions

References

Tables

Figures

⏪

⏩

◀

▶

Back

Close

Full Screen / Esc

Printer-friendly Version

Interactive Discussion

4.2 Time dependence

The time series showing the number of radionuclides in bottom sediment phase begins to increase around mid-April in SMIX (Fig. 8b), which is about a week later than CTRL (Fig. 8a). The accumulation speed is about half and the total number of radionuclides in bottom sediments is 0.24 PBq, which is also about half of CTRL (Fig. 8a, b). This reduction occurs because it takes longer time for the radionuclides to reach the bottom when the vertical mixing coefficient is small. So before depositions occur, the oceanic flow field has more time to advect the radionuclides offshore, where the topography is much deeper. It requires further time for radionuclides to transfer to bottom sediment phase in deeper locations and so the amount of deposition further reduces.

In SMIX, more radionuclides remain in dissolved phase compared to CTRL and moreover, they are dispersed to the open ocean. For SMIX, the amount of radionuclides in seawater that escape to where the bathymetry is deeper than 200 m is about 2.8 PBq in June. This suggests that 1.6 PBq more (or two times more) radionuclides are in the open ocean compared to CTRL. Such difference likely occurred because of less adsorption to bottom sediments and because more radionuclides remain near the surface where the flow field is much faster and able to move offshore. A decrease in vertical mixing therefore not only reduces the number of radionuclides that remain near the coast but also increases the number of radionuclides that rapidly disperses to the open ocean.

5 Summary and closing remarks

In this study, we investigated the impact of phase transfer on the dispersion of radionuclides that was released to the ocean from the FNPP. A Lagrangian particle-tracking model was used by coupling it to a numerical ocean model and by solving the phase transfer of radionuclides based on a stochastic method following Periañez (2000) and Kobayashi (2007). Many of the past studies have investigated the mechanism

BGD

10, 3677–3705, 2013

Oceanic dispersion of radionuclides along the coast of Fukushima

Y. Choi et al.

Title Page

Abstract

Introduction

Conclusions

References

Tables

Figures

⏪

⏩

◀

▶

Back

Close

Full Screen / Esc

Printer-friendly Version

Interactive Discussion



Oceanic dispersion of radionuclides along the coast of Fukushima

Y. Choi et al.

[Title Page](#)

[Abstract](#)

[Introduction](#)

[Conclusions](#)

[References](#)

[Tables](#)

[Figures](#)

[⏪](#)

[⏩](#)

[◀](#)

[▶](#)

[Back](#)

[Close](#)

[Full Screen / Esc](#)

[Printer-friendly Version](#)

[Interactive Discussion](#)

responsible for the dispersion of radionuclides from the FNPP but in absence of changes in phase. We consider three major phases of radionuclides; those dissolved in seawater (dissolved phase), those adsorbed in Large Particulate Matter (LPM phase), and those adsorbed in bottom sediments (bottom sediment phase). Here we summarize two major outcomes from our findings.

1. Significant amount of the adsorption to bottom sediments likely occurred within the first month or two. Therefore, the oceanic flow field during this period played an important role on determining the spatial distribution of radionuclides near the coast. For March 2011, the weak northward flow along the shelf-break and the westward surface Ekman transport kept many radionuclides to remain near the coast. This enhances the adsorption to bottom sediments and limited a rapid dispersion of radionuclides to the open ocean.
2. The amount of the radionuclides that are adsorbed to bottom sediments and that rapidly disperses to the open ocean depends on the magnitude of vertical mixing; smaller mixing leads to less deposition near the source and more dispersion to its surroundings and the open ocean. This is because vertical mixing slows the time the radionuclides need to reach the bottom, where deposition occurs.

It is worth noting at the end that there are obviously limitations to the model results we presented in this paper. First, there should be some differences between the flow fields simulated in our model from reality although we consider its general features reasonable. We do find the flow field sensitive to the lateral boundary condition, obviously because the region is affected by Kuroshio, one of the most energetic currents in the world. For example, the southward flow along the coast of Ibaraki that is simulated during the last few days of May in our model could be stronger and longer. This will enable more radionuclides to intrude to the southern coast of Ibaraki, enter the Kuroshio Extension, and disperse to the open ocean. Observations did show radionuclides in bottom sediments near the southern tip of Ibaraki and suggest some form of southward flow present at some time. Second, the number of radionuclides that are

Oceanic dispersion of radionuclides along the coast of Fukushima

Y. Choi et al.

[Title Page](#)

[Abstract](#)

[Introduction](#)

[Conclusions](#)

[References](#)

[Tables](#)

[Figures](#)

[⏪](#)

[⏩](#)

[◀](#)

[▶](#)

[Back](#)

[Close](#)

[Full Screen / Esc](#)

[Printer-friendly Version](#)

[Interactive Discussion](#)

adsorbed to bottom sediments are somewhat sensitive to the parameters we use in the particle-tracking model. Although the qualitative behaviors of the radionuclides we have shown in this study will likely to hold to the first order, multiple classes of particulate matters and two-step transfer models for bottom sediments (Perianez et al., 2012) may be needed for more realistic modeling of radionuclides. Third, we have not considered the impact of freshwater inputs from local rivers, which could limit vertical mixing through enhanced stratification. Inclusion of rivers may make the behavior of radionuclides along the coast of Fukushima resemble more like SMIX than CTRL. Further investigation on the impact of these features mentioned above on the behavior of radionuclides is beyond the scope of this study. But nonetheless, our study suggests the need to use models that incorporate the migration of radionuclides into different phases for more detailed understandings of their dispersion from the FNPP near the coast.

Acknowledgements. The authors thank M. Toratani for the satellite images from MODIS data used in Fig. 5, Y. Miyazawa for JCOPE2 data outputs, and the numerical modeling subgroup of the Oceanographic Society of Japan led by M. Ikeda for many discussions and inputs. Comments by anonymous reviewers greatly helped improve the paper, and we also thank T. Kobayashi, K.-S. Suh, and B.-I. Min for discussion in developing the radionuclide dispersion model.

References

- Amante, C. and Eakins, B. W.: ETOPO1 1 Arc-Minute Global Relief Model: Procedures, Data Sources and Analysis, NOAA Technical Memorandum NESDIS NGDC-24, 19 pp., March 2009.
- Bailly du Bois, P., Laguionie, P., Boust, D., Korsakissok, I., Didier, D., and Fiévet, B.: Estimation of marine source-term following Fukushima Dai-ichi accident, *J. Environ. Radioactiv.*, 114, 2–9, doi:10.1016/j.jenvrad.2011.11.015, 2012.
- Buesseler, K., Jayne, S. R., Fisher, N. S., Rypina, I. I., Baumann, H., Baumann, Z., Breier, C. F., Douglass, E. M., George, J., Macdonald, A. M., Miyamoto, H., Nishikawa, J., Pike, S. M., and

Oceanic dispersion of radionuclides along the coast of Fukushima

Y. Choi et al.

Title Page

Abstract

Introduction

Conclusions

References

Tables

Figures

⏪

⏩

◀

▶

Back

Close

Full Screen / Esc

Printer-friendly Version

Interactive Discussion

Yoshida, S.: Fukushima-derived radionuclides in the ocean and biota off Japan, *P. Natl. Acad. Sci. USA*, 109, 5984–5988, doi:10.1073/pnas.1120794109, 2012.

Choi, Y. J., Abe, A., and Takahashi, K.: Development of oil-spill simulation system based on the global ocean-atmosphere model, *Gas Trans. Water Surf.*, 6, 407–418, 2011.

Choi, Y., Takahashi, K., Abe, A., Nishio, S., and Sou, A.: Simulation of deepwater horizon oil spill using coupled atmosphere-ocean model, *J. Japan Inst. Mar. Eng.*, 48, 15–19, 2013.

Estournel, C., Bosc, E., Bocquet, M., Ulses, C., Marsaleix, P., Winiarek, V., Osvath, I., Nguyen, C., Duhaut, T., Lyard, F., Michaud, H., and Auclair, F.: Assessment of the amount of cesium-137 released into the Pacific Ocean after the Fukushima accident and analysis of its dispersion in Japanese coastal waters, *J. Geophys. Res.*, 117, C11014, doi:10.1029/2012JC007933, 2012.

Honda, M. C., Aono, T., Aoyama, M., Hamajima, Y., Kawakami, H., Kitamura, M., Masumoto, Y., Miyazawa, Y., Takigawa, M., and Saino, T.: Dispersion of artificial caesium-134 and -137 in the western North Pacific one month after the Fukushima accident, *Geochem. J.*, 46, 1–9, 2012.

Kawamura, H., Kobayashi, T., Furuno, A., In, T., Ishikawa, Y., Nakayama, T., Shima, S., and Awaji, T.: Preliminary numerical experiments on oceanic dispersion of ^{131}I and ^{137}Cs discharged into the ocean because of the Fukushima Daiichi nuclear power plant disaster, *J. Nucl. Sci. Technol.*, 48, 1349–1356, doi:10.1080/18811248.2011.9711826, 2011.

Kida, S.: The impact of open oceanic processes on the antarctic bottom water outflows, *J. Phys. Oceanogr.*, 41, 1941–1957, doi:10.1175/2011JPO4571.1, 2011.

Kobayashi, T., Otsuka, S., Togawa, O., and Hayashi, K.: Development of a non-conservative radionuclides dispersion model in the ocean and its application to surface cesium-137 dispersion in the Irish Sea, *J. Nucl. Sci. Technol.*, 44, 238–247, 2007.

Large, W. G. and Pond, S.: Open ocean momentum flux measurements in moderate to strong winds, *J. Phys. Oceanogr.*, 11, 324–336, 1981.

Masumoto, Y., Miyazawa, Y., Tsumune, D., Tsubono, T., Kobayashi, T., Kawamura, H., Estournel, C., Marsaleix, P., Lanerolle, L., Mehra, A., and Garraffo, Z. D.: Oceanic dispersion simulations of ^{137}Cs released from the Fukushima Daiichi nuclear power plant, *Elements*, 8, 207–212, doi:10.2113/gselements.8.3.207, 2012.

Ministry of Education, Culture, Sports, Science and Technology (MEXT): Monitoring information of environmental radioactivity level, available at: <http://radioactivity.mext.go.jp/en/>, 2012.

Oceanic dispersion of radionuclides along the coast of Fukushima

Y. Choi et al.

Title Page

Abstract

Introduction

Conclusions

References

Tables

Figures

⏪

⏩

◀

▶

Back

Close

Full Screen / Esc

Printer-friendly Version

Interactive Discussion

- Miyazawa, Y., Zhang, R., Guo, X., Tamura, H., Ambe, D., Lee, J.-S., Okuno, A., Yoshinari, H., Setou, T., and Komatsu, K.: Water mass variability in the western North Pacific detected in a 15-year eddy resolving ocean reanalysis, *J. Oceanogr.*, 65, 737–756, doi:10.1007/s10872-009-0063-3, 2009.
- 5 Miyazawa, Y., Masumoto, Y., Varlamov, S. M., Miyama, T., Takigawa, M., Honda, M., and Saino, T.: Inverse estimation of source parameters of oceanic radioactivity dispersion models associated with the Fukushima accident, *Biogeosciences Discuss.*, 9, 13783–13816, doi:10.5194/bgd-9-13783-2012, 2012a.
- 10 Miyazawa, Y., Masumoto, Y., Varlamov, S. M., and Miyama, T.: Transport simulation of the radionuclide from the shelf to open ocean around Fukushima, *Cont. Shelf Res.*, 50–51, 16–29, 2012b.
- Nuclear Emergency Response Headquarters (NERH), Government of Japan: Report of the Japanese Government to the IAEA Ministerial Conference in Nuclear Safety – The accident at TEPCO's Fukushima Nuclear Power Stations, 2011.
- 15 Periàñez, R.: Modelling the tidal dispersion of ^{137}Cs and $^{239,240}\text{Pu}$ in the English Channel, *J. Environ. Radioact.*, 49, 259–277, 2000.
- Periàñez, R. and Elliott, A. J.: A particle-tracking method for simulating the dispersion of non-conservative radionuclides in coastal waters, *J. Environ. Radioact.*, 58, 13–33, 2002.
- 20 Periàñez, R., Suh, K., and Min, B.: Local scale marine modeling of Fukushima releases. Assessment of water and sediment contamination and sensitivity to water circulation description, *Mar. Pollut. Bull.*, 64, 2333–2339, 2012.
- Tokyo Electric Power Corporation (TEPCO): Detection of radioactive materials from the seawater around the discharge canal of Fukushima Daiichi Nuclear Power Station, Press Release, available at: <http://www.tepco.co.jp/en/nu/fukushima-np/f1/index2-e.html>, 2011.
- 25 Tsumune, D., Tsubono, T., Aoyama, M., and Hirose, K.: Distribution of oceanic ^{137}Cs from the Fukushima Dai-ichi Nuclear Power Plant simulated numerically by a regional ocean model, *J. Environ. Radioact.*, 111, 100–108, doi:10.1016/j.jenvrad.2011.10.007, 2011.
- Van Raaphorst, W., Philippart, C. J. M., Smit, J. P. C., Dijkstra, F. J., and Malschaert, J. F. P.: Distribution of suspended particulate matter in the North Sea as inferred from NOAA/AVHRR reflectance images and in situ observations, *J. Sea Res.*, 39, 197–215, 1998.
- 30 Yasuda, I.: Hydrographic structure and variability in the Kuroshio-Oyashio transition area, *J. Oceanogr.*, 59, 389–402, doi:10.1023/A:1025580313836, 2003.

BGD

10, 3677–3705, 2013

Oceanic dispersion
of radionuclides
along the coast of
Fukushima

Y. Choi et al.

Title Page

Abstract

Introduction

Conclusions

References

Tables

Figures



Back

Close

Full Screen / Esc

Printer-friendly Version

Interactive Discussion

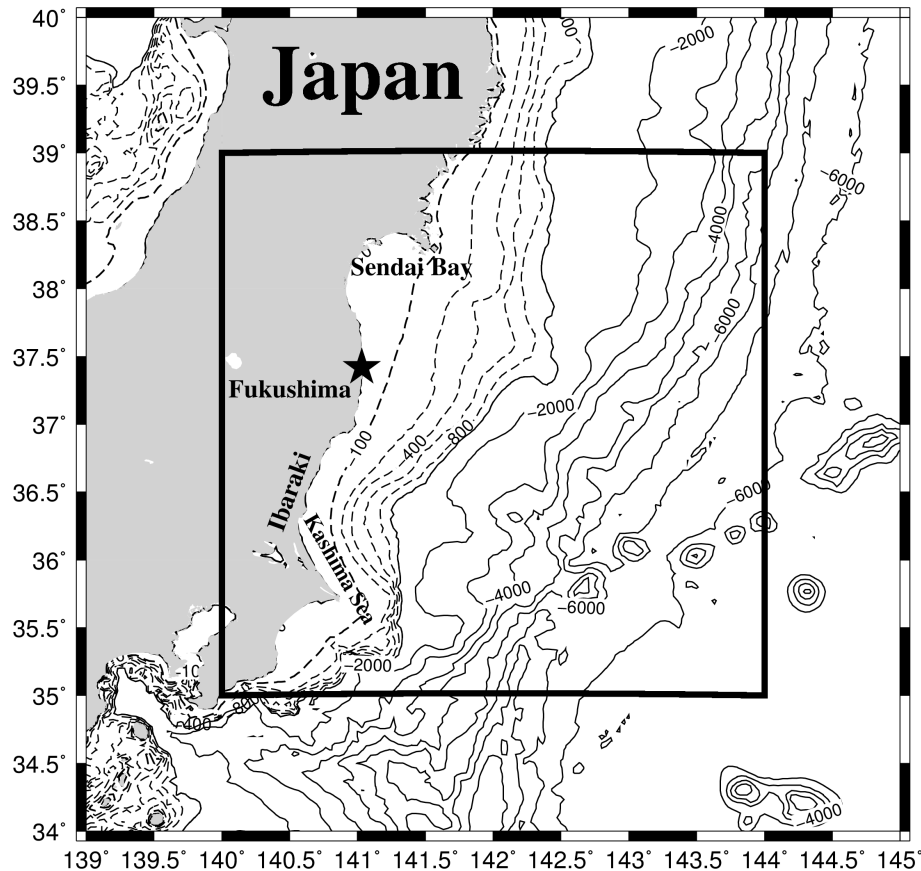


Fig. 1. Bottom topography of the region close to the FNPP. Contours are drawn for 100, 200, 400, 600, 800, 1000 m, and every 1000 m after that. Black star indicates the location of the FNPP. Model domain is the squared region surrounded by the thick black solid line. The continental shelf break, which can be roughly interpreted from the 200 m contour line, is located close to the coast near Ibaraki but further off-shore near Fukushima.

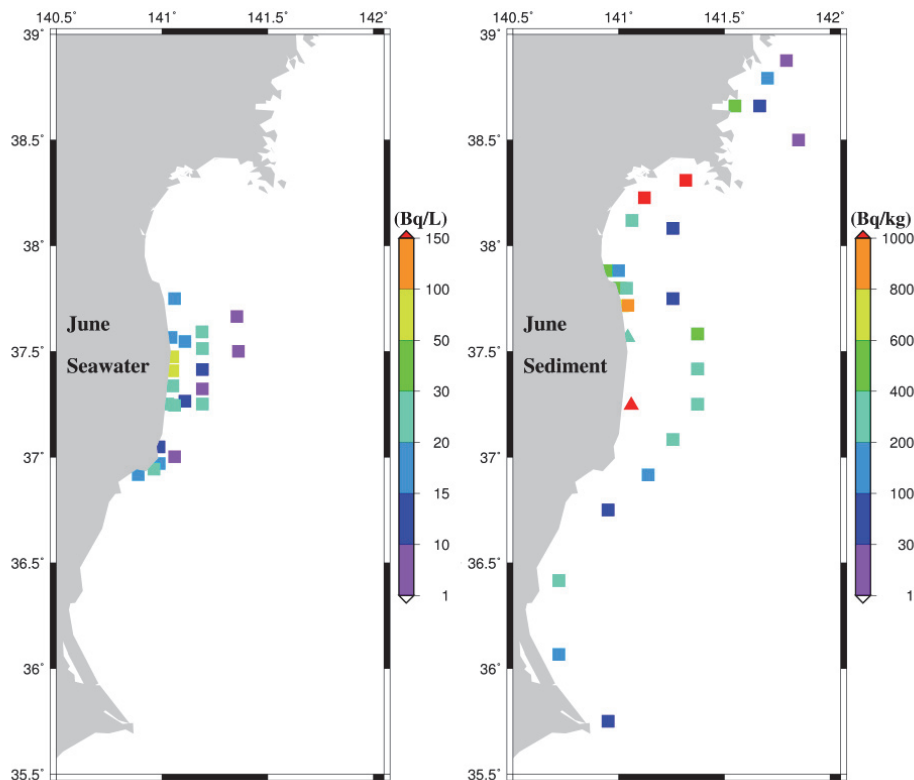


Fig. 2. Concentrations of radionuclides in **(a)** Seawater [Bq L^{-1}] and **(b)** bottom sediments [Bq kg^{-1} dry] observed in June 2011 (MEXT, 2011). Note that data from TEPCO are measured in [Bq kg^{-1} wet] and are shown in triangles. The values are also converted to [Bq kg^{-1} dry] by multiplying by 0.75 (MEXT, 2011). Higher levels of radionuclides are observed near the FNPP and also along the coast from the southern tip of Ibaraki to the Sendai Bay.

Oceanic dispersion of radionuclides along the coast of Fukushima

Y. Choi et al.

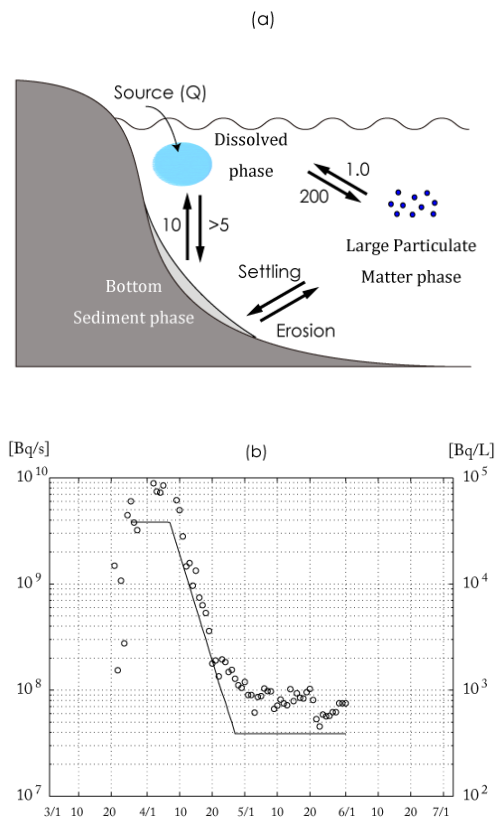


Fig. 3. (a) A schematic showing the three phases solved by the particle-tracking model along with the time scale of the phase transfer in [days]. Radionuclides are first introduced in dissolved phase. **(b)** Time series of the ^{137}Cs source term based on Tsumune et al. (2012) are shown in a black solid line ($[\text{Bq s}^{-1}]$, left axis). Observed concentrations at the outlet of Daiichi FNPP (TEPCO, 2011) are shown in a black circles ($[\text{Bq L}^{-1}]$, right axis).

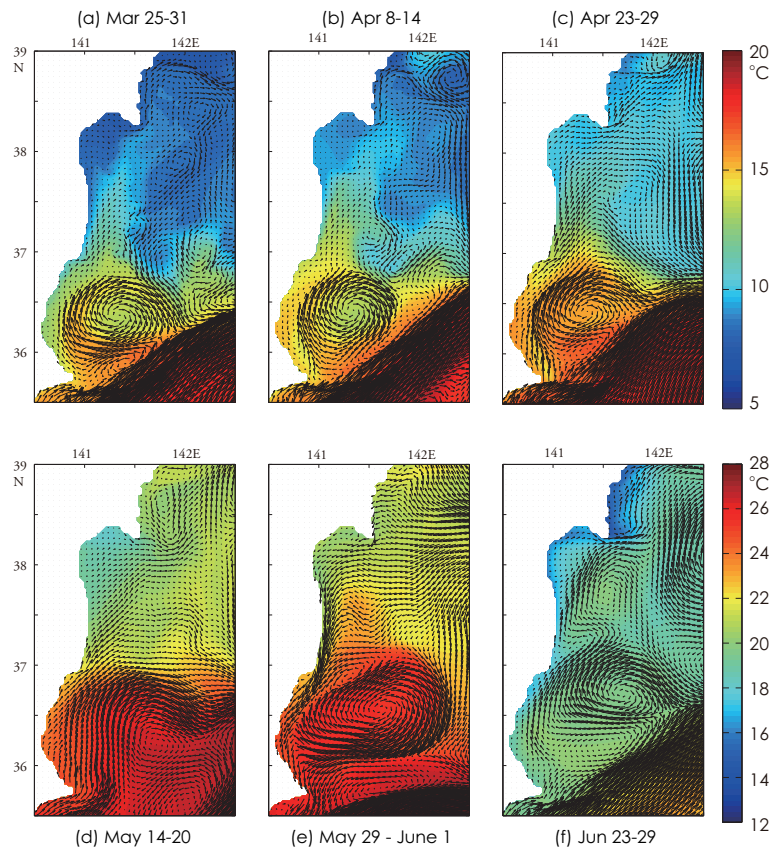


Fig. 4. Simulated flow fields and the SST for CTRL. **(a)** 25–31 March, **(b)** 8–14 April, **(c)** 23–29 April, **(d)** 14–20 May, **(e)** 29 May–1 June and **(f)** 23–29 June 2011. Color contours are shown on the top right for **(a–e)** but bottom right for **(f)**. The color contour is different for **(f)** so that it is similar to Fig. 5f.

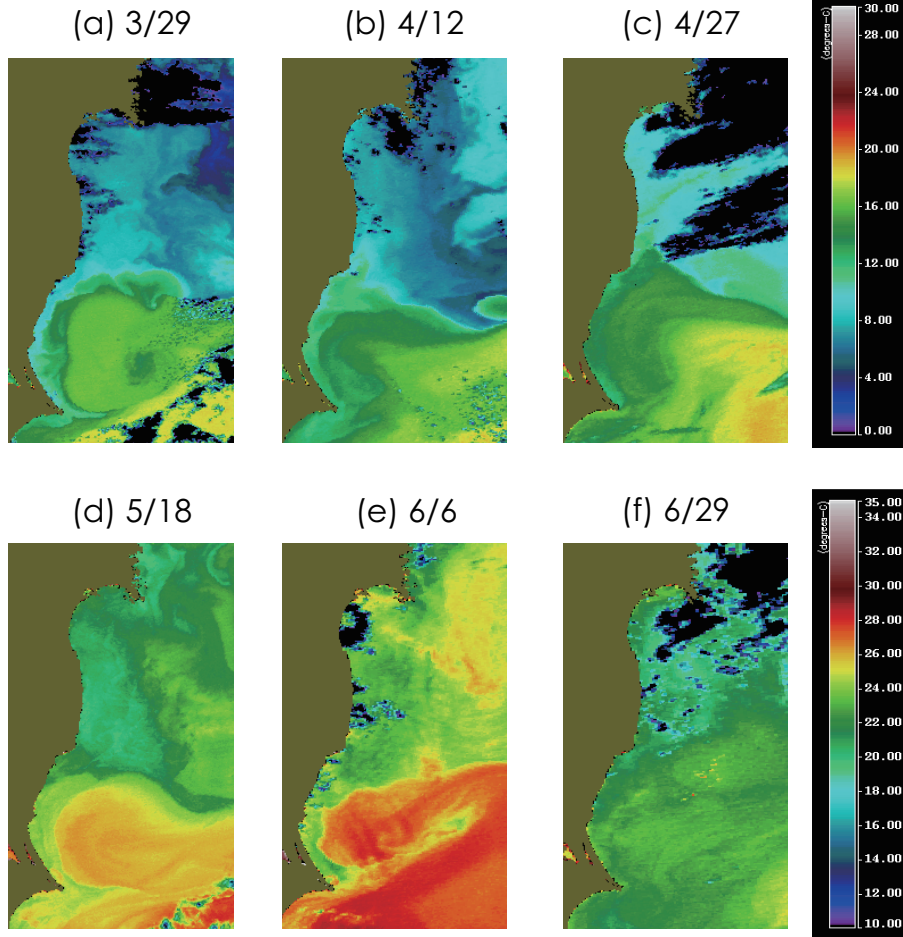


Fig. 5. The SST observed by MODIS from March to June 2011. Dark regions are where clouds exist. Color contours are shown on the top right for (a)–(e) but bottom right for (f).

Oceanic dispersion of radionuclides along the coast of Fukushima

Y. Choi et al.

Title Page

Abstract

Introduction

Conclusions

References

Tables

Figures

⏪

⏩

◀

▶

Back

Close

Full Screen / Esc

Printer-friendly Version

Interactive Discussion



Oceanic dispersion of radionuclides along the coast of Fukushima

Y. Choi et al.

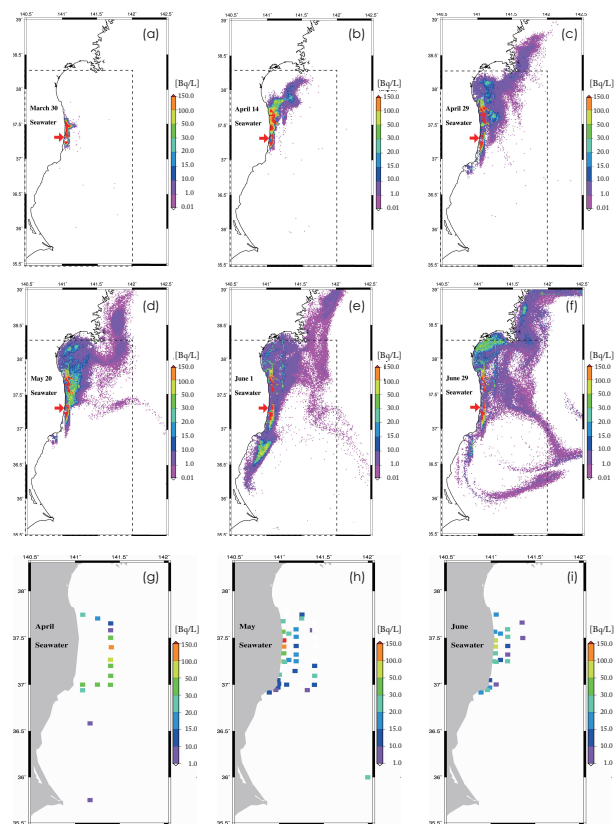


Fig. 6. (a–f) Radionuclide concentrations in seawater (dissolved and LPM phases) in CTRL: (a) 30 March, (b) 14 April, (c) 29 April, (d) 20 May, (e) 1 June, and (f) 29 June 2011. (g–i) Monthly averages of observed radionuclide concentration in seawater: (g) April, (h) May, and (i) June 2011.

[Title Page](#)
[Abstract](#)
[Introduction](#)
[Conclusions](#)
[References](#)
[Tables](#)
[Figures](#)
[Back](#)
[Close](#)
[Full Screen / Esc](#)
[Printer-friendly Version](#)
[Interactive Discussion](#)

Oceanic dispersion of radionuclides along the coast of Fukushima

Y. Choi et al.

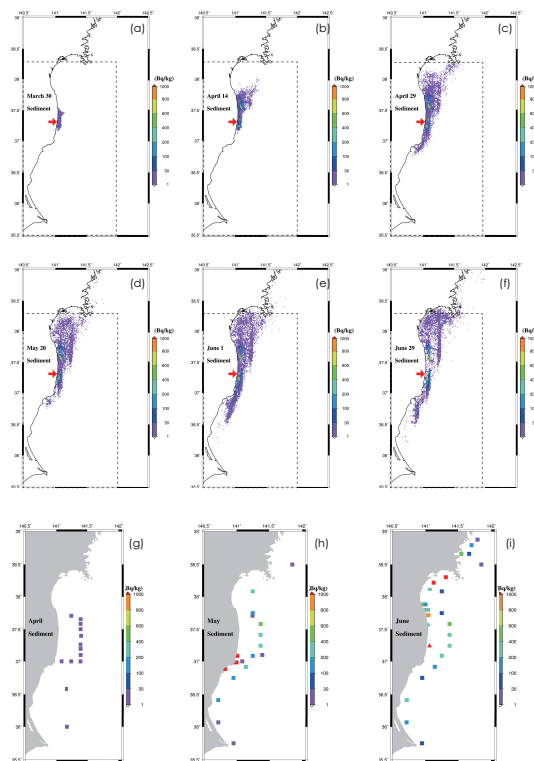


Fig. 7. (a–f) Radionuclide concentration in bottom sediment phase in CTRL [Bq kg^{-1} dry]: (a) 30 March, (b) 14 April, (c) 29 April, (d) 20 May, (e) 1 June, and (f) 29 June 2011. (g–i) Monthly averages of observed radionuclide concentration in bottom sediments: (g) April, (h) May, and (i) June 2011. Note that data from TEPCO are measured in [Bq kg^{-1} wet] and are shown in triangles. The values are also converted to [Bq kg^{-1} dry] by multiplying the value by 0.75 (MEXT, 2011).

[Title Page](#)
[Abstract](#)
[Introduction](#)
[Conclusions](#)
[References](#)
[Tables](#)
[Figures](#)
[Back](#)
[Close](#)
[Full Screen / Esc](#)
[Printer-friendly Version](#)
[Interactive Discussion](#)

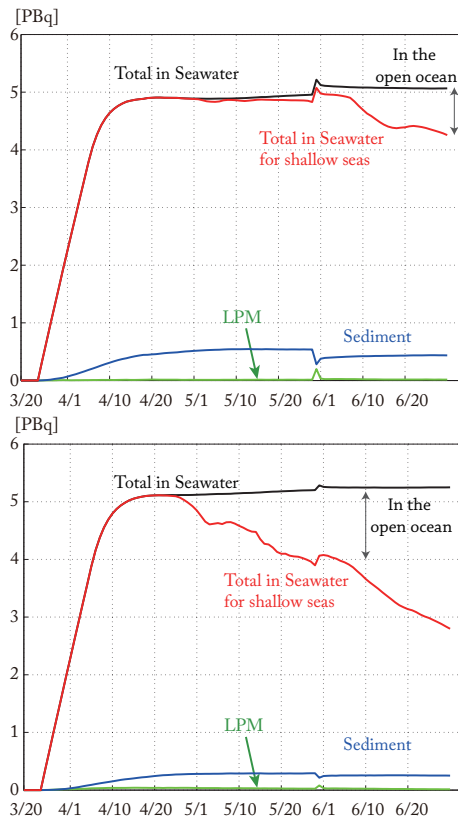


Fig. 8. (a) Time series of radionuclides in CTRL. **(b)** Time series of radionuclides in SMIX. Green and blue lines show the radionuclides in LPM phase and bottom sediment phase, respectively. Black solid line is the sum of radionuclides in dissolved and LPM phases including those that exited from the model domain. Red line is the sum of radionuclides in dissolved and LPM phases that are located in shallow seas (< 200 m). The difference between the black and red lines is the number of radionuclides in the open ocean (> 200 m).

Oceanic dispersion of radionuclides along the coast of Fukushima

Y. Choi et al.

Title Page

Abstract Introduction

Conclusions References

Tables Figures

⏪ ⏩

◀ ▶

Back Close

Full Screen / Esc

Printer-friendly Version

Interactive Discussion



Oceanic dispersion of radionuclides along the coast of Fukushima

Y. Choi et al.

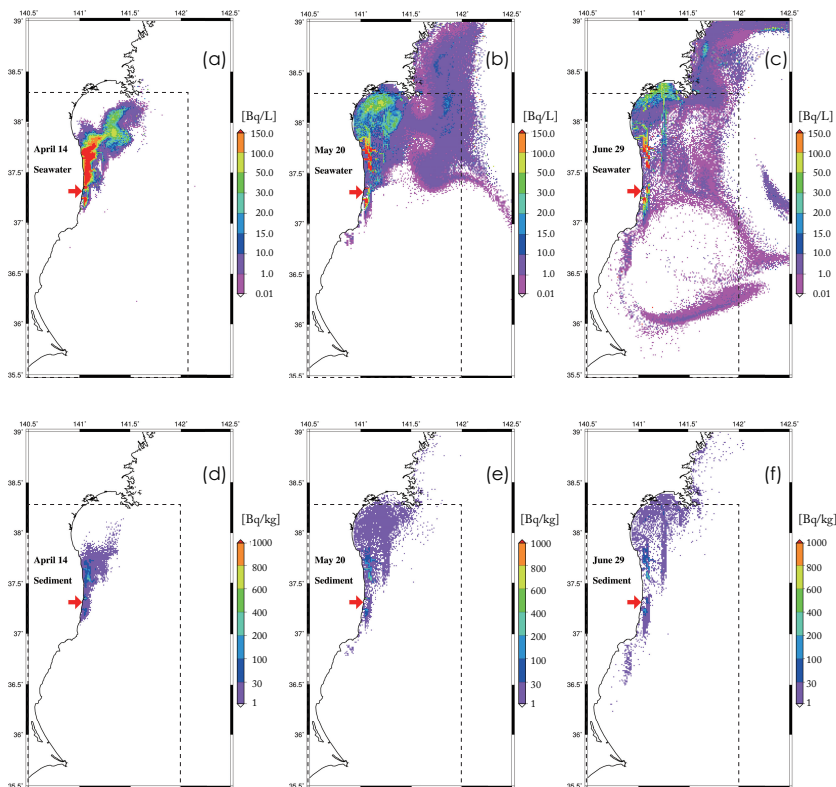


Fig. 9. Model results of SMIX. Radionuclide concentration in seawater phase (dissolved and LPM phases): **(a)** 14 April, **(b)** 20 May, **(c)** 29 June 2011. **(d–f)** Radionuclide concentration in bottom sediment phase: **(d)** 14 April, **(e)** 20 May, **(f)** 29 June 2011.

Title Page

Abstract

Introduction

Conclusions

References

Tables

Figures

⏪

⏩

◀

▶

Back

Close

Full Screen / Esc

Printer-friendly Version

Interactive Discussion